HNPS Advances in Nuclear Physics

Vol 2 (1991)

HNPS1991

INCLUSIVE PRODUCTION OF INTERMEDIATE MASS FRAGMENTS IN 20Ne+Ag,Au INTERACTIONS AT 20-60 MeV/nucleon

N. H. Papadakis, - et al.

doi: 10.12681/hnps.2842

INCLUSIVE PRODUCTION OF INTERMEDIATE MASS FRAGMENTS IN ^{20}Ne+Ag,Au INTERACTIONS AT 20-60 MeV/nucleon

N.H.PAPADAKIS[1]*, N.P.VODINAS[1], Y.CASSAGNOU[2], R.DAYRAS[2], R.FONTE[3], G.IMME[3], R.LEGRAIN[2], A.D.PANAGIOTOU[1], E.C.POLLACCO[2], G.RACITI[3], L.RODRIGUEZ[2], F.SAINT-LAURENT[4], M.G.SAINT- LAURENT[4] and N.SAUNIER[2]

[1] Physics Department, Nuclear and Particle Physics Division. University of Athens. Panepistimiopolis, GR-15771 Athens, Greece

[2] Department de Physique Nucleaire - S.E.P.N., C.E.N. Saclay, F-91191 Gif-sur-Yvette Cedex, France

[3] INFN-LNS and Physics Department, University of Catania. 57 Corso Italia, I-95129 Catania, Italy

[4] GANIL, B.P.5027, F-14021 Caen Cedex, France

Abstract

Energy spectra and angular distributions of intermediate mass fragments were measured in ^{20}Ne interactions with Ag and Au targets at 20, 30, 40, 50 and 60 MeV/nucleon incident energies. Assuming two prevailing origins, fragmentation and evaporation (or fission), the measured energy spectra and angular distributions are reproduced by emission from

*Presented by N.H.Papadakis

two moving sources. The dependence of the parameters extracted for the sources on the fragment charge and on the incident energy is discussed. The distinctive role of fission in the case of the gold target is stressed. Nuclear fragmentation cross sections deduced from the moving source analysis are given and discussed for the two systems.

1 Introduction

The study of intermediate mass fragments (IMF), emitted in nucleus-nucleus interactions in the energy range from 20 to 100 MeV/nucleon where the relative velocity is commensurable with the velocity of sound and Fermi velocity in nuclear matter, has been of particular interest in the last few years[1]. In this energy domain, the emission of complex fragments, in the range $5 \leq Z \leq 20$, in processes different from binary fission, has been the subject of intense theoretical investigations. At present, there is no consensus as to the origin of these fragments; however their production is expected to depend on the bombarding energy, the mass of the system and perhaps on other dynamical quantities, and to be connected with the most dissipative reactions at intermediate and central impact parameters.

Statistical as well as dynamical models have been proposed to explain the emission mechanism of IMF [1]. These models differ in rather basic assumptions concerning the size, density, internal excitation and degree of thermalization of the emitting system as well as in the way this emitting system breaks or decays.

In order to get evidence of the change in fragmentation regime, it was considered necessary to systematically and consistently study with good statistics the dependence of inclusive complex fragment cross sections on the bombarding energy. This is performed here for an intermediate mass (Ne+Ag) and a heavy mass (Ne+Au) system in a large incident energy range covering 20 to 60 MeV/nucleon. These broad-base data shed light on the possible mechanism(s) for the emission of complex fragments as a function of the available energy and the size of the system.

2 Parametrization with moving sources

The energy spectra at the measured angles were parametrized for each fragment assuming two moving sources: a fast source simulating nuclear fragmentation and a slow source reproducing the yield from evaporation and fission of target-like nuclei.

One should in principle have added a third source to fit the contribution from the de-excitation of projectile-like nuclei at very forward angles. This contribution was taken into account for fragments lighter than the projectile by introducing a cut in the high energy tail of the spectra measured at the most forward angles (θ <25 deg.). Secondary de- excitation processes which mainly contribute to the production of light nuclei with Z<5, are neglected in this analysis, concentrated on Z- separated heavier fragments.

2.1 Fitting procedure

The energy spectra at the various angles of fragments having a given Z are fitted by the following expression:

$$\frac{d^2\sigma(\theta)}{d\Omega dE} = \frac{d^2\sigma(\theta)}{d\Omega dE_{(f)}} + P\frac{d^2\sigma(\theta)}{d\Omega dE_{(evf)}} \qquad (1)$$

where (f) stands for fragmentation and (evf) for evaporation and fission. All processes different from these latter relaxed ones are thus considered as fragmentation.

In eq. (1),

$$\frac{d^2\sigma(\theta)}{d\Omega dE_{(f)}} = [E-E_{c(f)}]^{\frac{1}{2}} exp\left(-\frac{E - E_{c(f)} + E_{s(f)} - 2(E - E_{c(f)})^{1/2}E_{s(f)}^{1/2}cos\theta}{T_{(f)}}\right) \qquad (2)$$

represents a non-relativistic Maxwell-Boltzman-type distribution of probabilities for finding a fragment of mass A, charge Z, with lab. energy E, at lab. angle θ in dE and $d\Omega(\theta)$ intervals, as a function of the source

temperature $T_{(f)}$ and velocity $v_{s(f)}$ with

$$v_{s(f)} = \left(\frac{2E_{s(f)}}{Am_0}\right)^{\frac{1}{2}} \tag{3}$$

and m_0=931.478 MeV. $E_{c(f)}$ is a Coulomb correction to the lab. energy accounting for the repulsion from the target remnant charges in the fragmentation process.

The second term of eq. (1) is given by:

$$\frac{d^2\sigma(\theta)}{d\Omega dE_{(evf)}} = E^{\frac{1}{2}} exp\left[-\frac{U}{T_{(evf)}}\right]\left[1 + exp\left(\frac{E_{c(evf)} - U}{D}\right)\right]^{-1} \tag{4}$$

with

$$U = E + E_{s(evf)} - 2E^{\frac{1}{2}}E_{s(evf)}^{\frac{1}{2}}cos\theta \tag{5}$$

which is similar in shape to eq. (2), with $T_{(evf)}$ being the temperature of the nucleus which undergoes fission or evaporates nucleons (and light nuclei) while

$$v_{s(evf)} = \left(\frac{2E_{s(evf)}}{Am_0}\right)^{\frac{1}{2}} \tag{6}$$

is its recoil velocity. The Coulomb term $E_{c(evf)}$ is not substracted from E as in eq. (2) but is introduced in a subthreshold penetration coefficient having a width D taken as 1 MeV.

Complete and incomplete fusion being most probable in central collisions [2], the source allowing for evaporation and fission (having A_{tot} nucleons and Z_{tot} protons) can be expected close in size to the compound or target nucleus (both are considerably heavier than the projectile in the present case). $E_{c(evf)}$ should then approach the Coulomb barrier:

$$E_{c(max)} = \frac{e^2Z(Z_{tot} - Z)}{r_0[A^{\frac{1}{3}} + (A_{tot} - A)^{\frac{1}{3}}]} \tag{7}$$

between two touching spheres, while $E_{c(f)}$ could be lower, as a result of a possible small number of remnant charges.

The parameter P in eq. (1) determines the relative intensity of the two sources. Normalization to the data gives absolute cross sections for

each source. Seven parameters ($T_{(f)}$, $v_{(f)}$, $E_{c(f)}$, $T_{(evf)}$, $v_{(evf)}$, $E_{c(evf)}$, P) are therefore necessary to fit the energy spectra of one fragment at the different angles with eqs. (1),(2) and (4). An example of fit to the double differential cross sections is given by solid curves in fig. 1.

2.2 Intermediate velocity source

In fig. 2a. the temperatures $T_{(f)}$ of the intermediate velocity source in Ne+Ag and Ne+Au as a function of the charge (size) of the fragment are compared at different energies. For the two targets, the temperature shows a constant or increasing trend for $Z < Z_{beam}$ followed by a rapid fall-off for higher Z- values.

It is now accepted that the parameters $T_{(f)}$ extracted from the slopes of kinetic energy spectra do not provide good measurements of source temperatures[3]. Moreover these slope parameters which decrease with the mass of the fragments may appear at variance with the idea of an equilibrated emitting system unique for all fragments. The slopes of the energy spectra are however related to the true temperature because a linear dependence results from momentum conservation between the measured temperature and the fragment mass, if the source has a limited number of nucleons. According to ref. [3], if T is the temperature of a system of A_{total} nucleons, one should measure an apparent temperature $T_{(f)}$ which can be approximated, for fragments having a large enough mass A by:

$$T_{(f)} = T\left(1 - \frac{A}{A_{total}}\right) \tag{8}$$

Applying eq. (8) to the variation of $T_{(f)}$ for $Z > 10$ observed in fig. 2a source sizes of $\simeq$75 nucleons in Ne+Ag and $\simeq$130 nucleons in Ne+Au can be estimated. True temperatures of 25 and 20 MeV are further extrapolated for the reactions on silver and gold, respectively.

The observed decrease versus Z of the slope parameter has been previously explained by assuming that heavier fragments could be emitted at a later stage of the cooling down when the source has reduced degrees of freedom for decay or that the source could evolve through an expansion

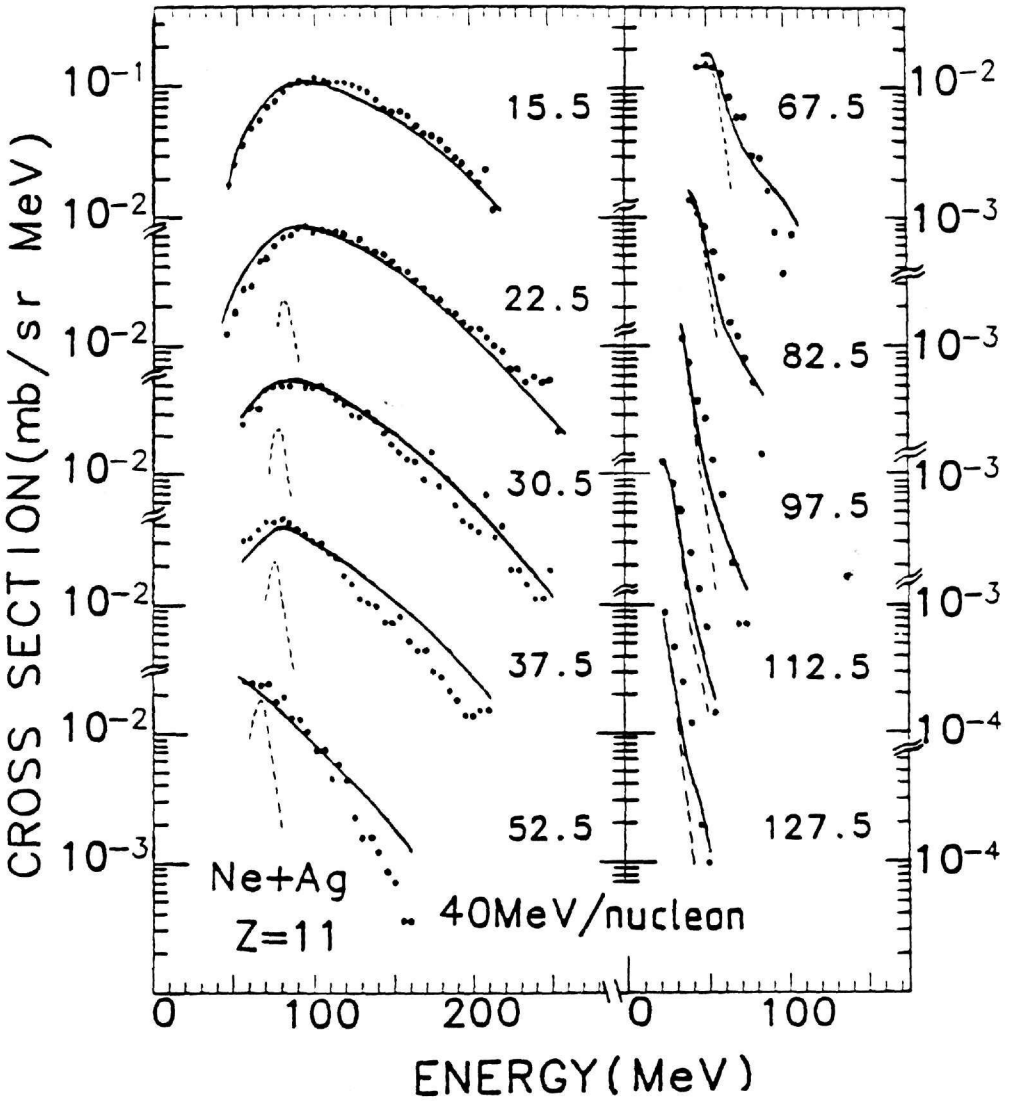

Figure 1: Energy spectra of Z=11 fragments from Ne+Ag at 40 Mev/nucleon as a function of the lab. angle. Solid curves show fits with two moving sources. The dashed lines represent the only evaporation component.

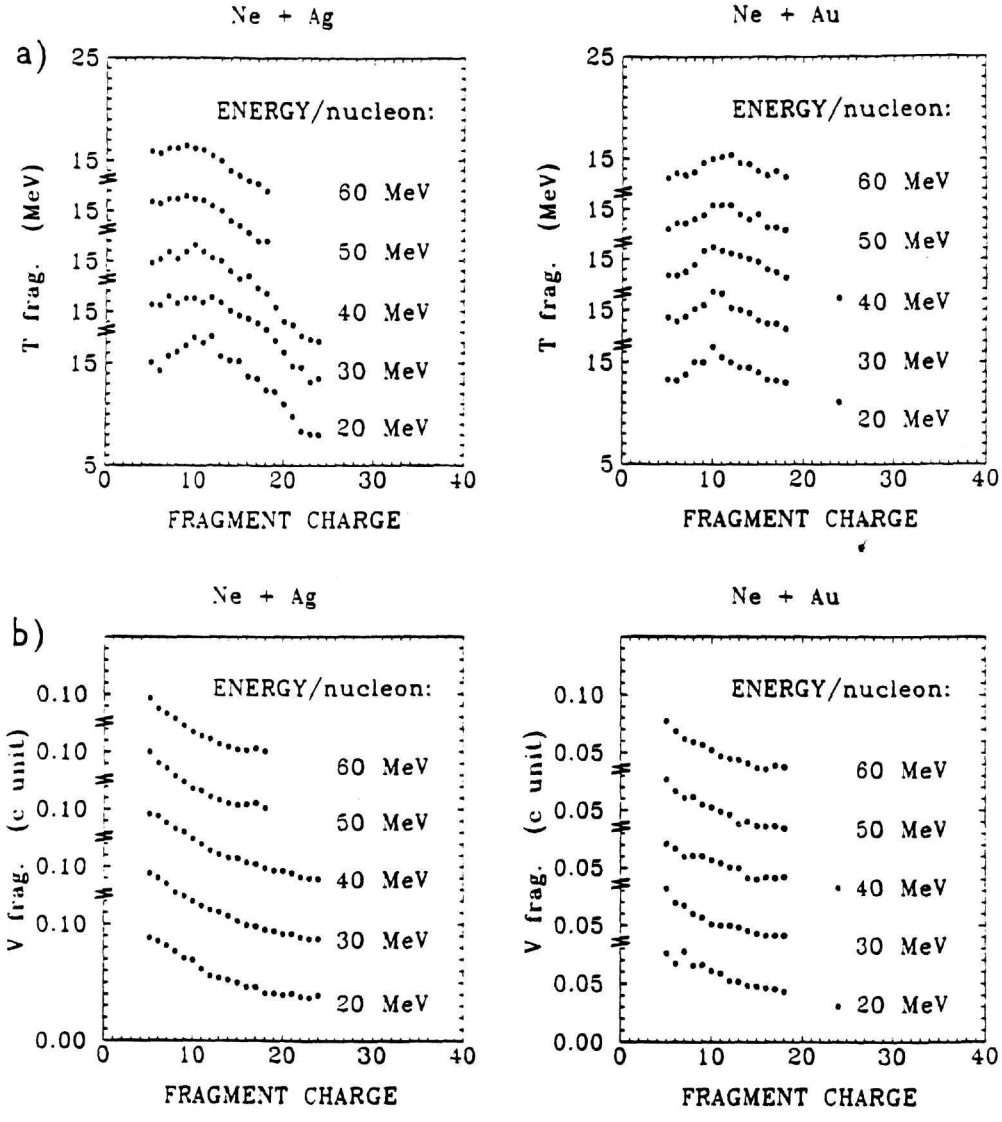

Figure 2: Temperature and velocity parameters of the intermediate-velocity source as a function of the fragment Z for Ne+Ag and Ne+Au between 20 and 60 MeV/nucleon.

inside the target spectator (accretion): more nucleons being progressively involved in the source, the temperature would decrease and larger fragments be emitted.

The source velocity appears in fig. 2b similarly decreasing as a function of Z for both targets, even for light fragments. If one relates the source velocity to its dimension by simply using momentum conservation[4], the light fragments which are assigned to a source half as fast as the projectile would thus originate from a set of equal number of target and projectile nucleons, whereas the source for the heaviest fragments, found two times slower, would be roughly double in size. The hypothesis of accretion[4] could thus appear to successfully account for the decreasing trend of both temperature and velocity with Z.

A better explanation may be given by considering impact parameters: one may expect that the large velocities and temperatures associated with the lighter fragments are related to small impact parameters i.e. large momentum and energy transfers from the projectile. Heavy fragments, in the same view, would be coming from more gentle collisions involving smaller momentum transfers. In very asymmetric reactions like Ne+Ag and Ne+Au, the source size can be expected independent of the impact parameter till the latter reaches some value[2]. Beyond this limit binary processes which are dominant in central collisions (e.g. fusion + sequential evaporation or/+ fission) would compete with fragmentation into light nuclei. As the impact parameter increases further (with reduced energy/momentum transfer), less fragments having greater sizes would result from fragmentation, ending with only two fragments indistinguishable from those of the simple fission induced in peripheral collisions. In support of this scheme, arguments can be given from simple geometry which predict enlarged sources for greater impact parameters[2]. Reduced temperatures and velocities then follow. The present data are unfortunately limited to $Z \leq 24$ and therefore can only suggest that the source parameters found for the heavier fragments could reach values which, in the following subsection, will characterize equilibrated sources. Thus the reliability of the impact parameter explanation cannot be fully established.

2.3 Evaporation/Fission source

The parameters of the slow sources for fragments coming from evaporation and fission have been found, in the analysis, rather insensitive to the fragment charge (fig. 3); the temperature furthermore appears insensitive to the beam energy. This is in sharp contrast with the strong dependence on Z of the previous mid-velocity source parameters.

Slow sources associated with evaporated light nuclei of fission fragments from the Ne+Ag system, have a nearly constant temperature of 4.2 MeV (fig. 3a-right side) and a velocity which is significantly lower than the c.m. one: from $\frac{2}{3}v_{c.m.}$ at 20 MeV/nucleon to $\frac{1}{2}v_{c.m.}$ at 50 MeV/nucleon (fig. 3b). Incomplete fusion is a possible explanation in the case of evaporation of light nuclei. With regard to the heavier fragments in this experiment ($18 \leq Z \leq 24$) which may originate from fission as well as from evaporation, one can remark that they can be emitted in anyone of these processes after a large primordial emission of fast particles and light nuclei. This is characteristic of central collisions where a great amount of the deposited energy is carried away by a large number of energetic forward emitted nucleons. A nucleus of reduced size and speed remains having, as one can anticipate, a large deformation leading to an increased probability for asymmetric fission.

With the gold target, the temperature is nearly 4.3 MeV at all incident energies, and the mean velocity is equal to the c.m. velocity (β= 0.02c, 0.025c, 0.03c at 20, 40 and 60 MeV/nucleon, respectively) (fig. 3). There are possible indications of smaller velocities for the fragments with $Z > 18$ (the fits for Z=24 at 20-40 MeV/nucleon give hints for $v_{(evf)}$ values 20% lower than the c.m. velocity).

The contribution of the slow source in energy spectra is illustrated on fig. 1 in the case of Z=11 fragments for Ne+Ag at 40 MeV/nucleon. This contribution amounts to nearly all the yield at the backward angles (see spectra at 112.5^0 and 127.5^0). It is still important in the low energy region at intermediate angles and is almost negligible at forward angles.

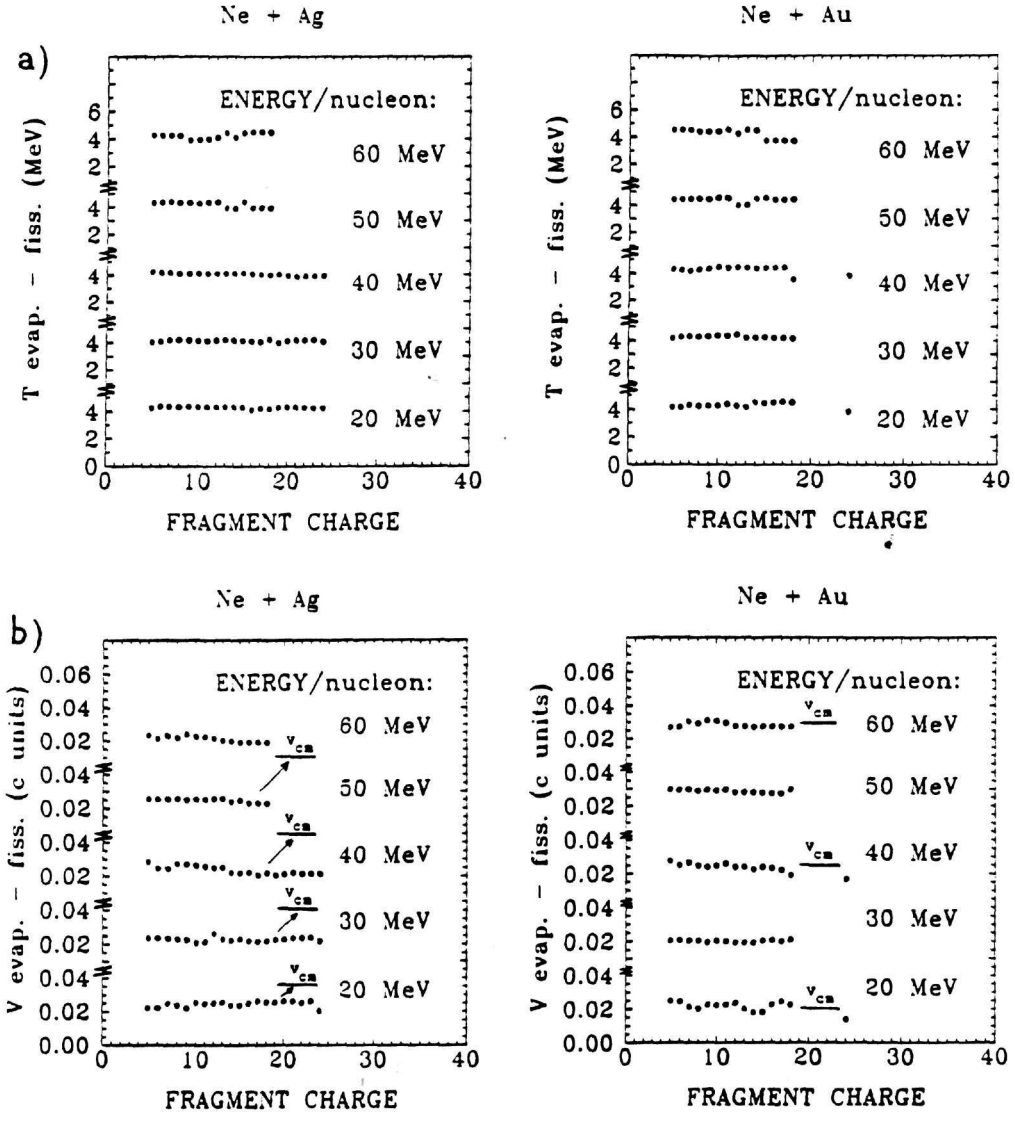

Figure 3: Temperature and velocity parameters of the evaporation/fission source as a function of the fragment Z for Ne+Ag and Ne+Au between 20 and 60 MeV/nucleon.

2.4 Coulomb corrections

The dependence on Z of the Coulomb correction terms $E_{c(evf)}$ and $E_{c(f)}$ is shown in fig. 4. For the two studied targets, one observes an approximately linear increase of both these parameters with Z, but apparently too weak increase for a unique fission-evaporation/fragmentation source to be relevant for all fragments.

As an example, the parameter of the slow source, $E_{c(evf)}$, is for the lightest fragments very close to the Coulomb repulsion between two spheres in contact including all the nucleons and charges of the reaction i.e. using eq. (7). It is what one would expect in central collisions from fusion-evaporation processes. Eq. (7) applied to the heavy fragments predict for both targets a too large Coulomb correction (see dashed curves in fig. 4b at 20 MeV/nucleon). By assuming a pre- emission of about 15 energetic nucleons at the projectile velocity, one gets a better agreement for silver (dash-dotted line). A similar fit to the gold data would require 50 nucleons to be removed by pre-equilibrium emission, which is not acceptable.

In asymmetric fission, fragments are released at increased distances by deformed nuclei. Deformation could thus better explain the small values of $E_{c(evf)}$ found for the large fragments of gold in this analysis. Solid lines in fig. 4b show predictions according to Viola[5] for both targets: for the heaviest fragments of silver, E_c values extracted at 20 MeV/nucleon are fairly well approximated while, for gold, an agreement appears possible only if preliminary nucleon emission is again assumed.

The Coulomb term of the intermediate velocity source, $E_{c(f)}$, is, for light nuclei, 40% lower than the above slow source term. Contrary to evaporation, fragmentation in the case of a simultaneous break-up can occur at distances shorter than the summed radii of the fragment and remnant nuclei. For instance, if a nucleus (Ag or Au) breaks into three clusters of equal sizes when at the same time a fourth light fragment is emitted, the kinetic energy gained by the latter from the Coulomb repulsion can be smaller than what is predicted in the case of successive evaporation events taking place at the nuclear surface. The reduced Coulomb terms observed in this analysis are consistent with a multifragmentation of the

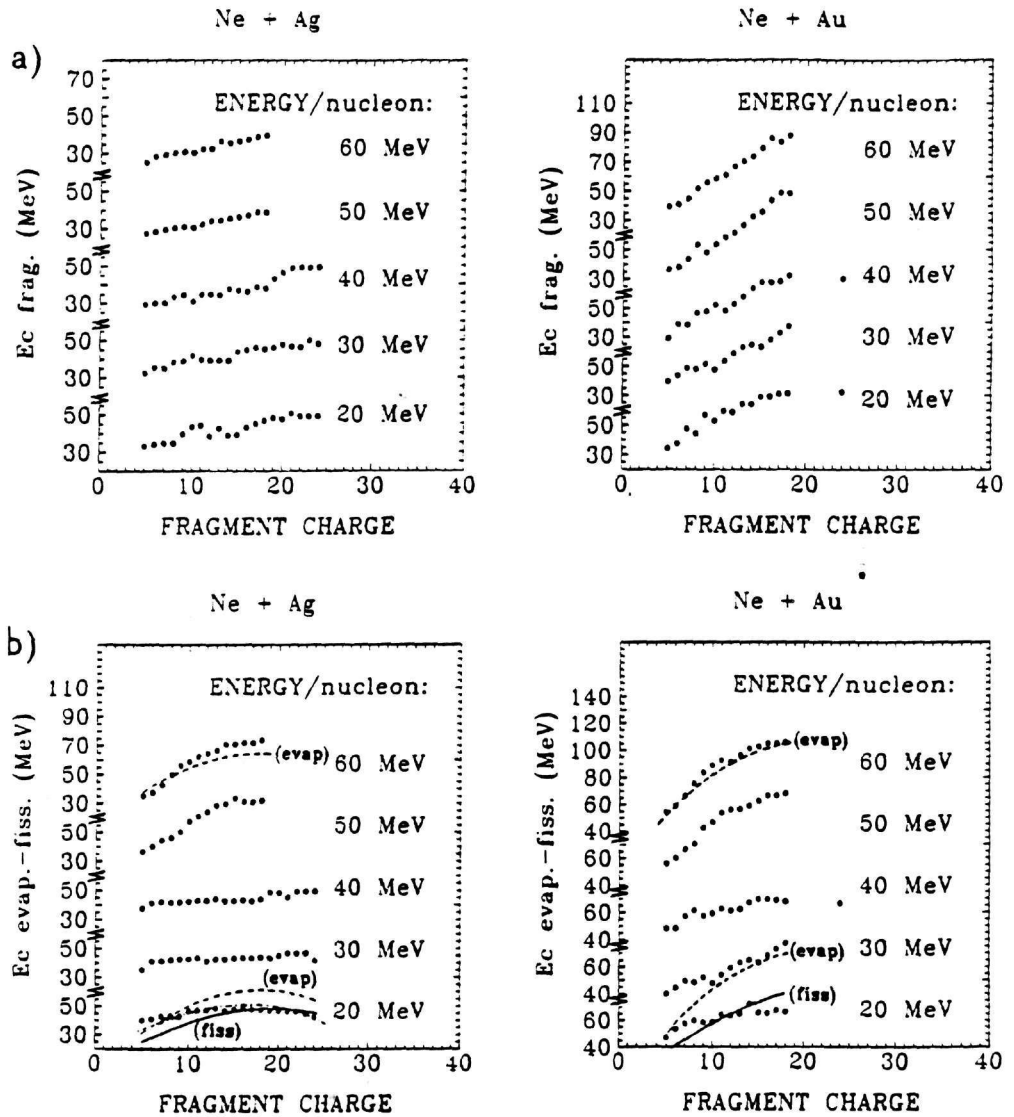

Figure 4: Dependence of the Coulomb corrections on the fragment charge for Ne+Ag and Ne+Au between 20 and 60 MeV/nucleon. Curves are explained in the text.

whole target[6,7]. The non-sequential nature of the process yielding mid-velocity fragments can be evidenced by measuring the relative velocities of correlated fragments[8].

For the heaviest fragments. $E_{c(f)}$ gets close to the slow source value. One indeed can predict smaller number of fragments in the case of large Z values and thus reduced differences between fragmentation and fission in Coulomb effects. Proportionality to a part of the charge Z is again observed. Possible explanations are an expansion of the nucleus prior to its fragmentation or a deformation as above in the case of fission.

As a whole, despite larger uncertainties and a somewhat smoother trend for gold at 50 and 60 MeV/nucleon, the two Coulomb parameters show nearly complete independence on beam energy, as it was already the case for the temperature and velocity parameters.

2.5 Angular distributions

The angular distributions in the laboratory are all strongly forward peaked in particular for the lighter elements and for the higher energies. A detailed analysis can be found in ref. [9,10,11]. Examples of unfolding into components from a fast and a slow source are presented on fig. 5. As shown by dashed lines in fig. 5, the fast source gives a forward peaked component with a rise on approximately three decades for silver and two decades for gold in the studied angular range. On the contrary, the evaporation/fission source component (dotted lines) is rather flat with only a small increase of a factor of 2 to 4 in the same angular domain. Comparing the different energies, one sees that the angular distribution is dominated by a fast source component at high energy (see for example Ag and Au at 60 MeV/nucleon in fig. 5), whereas the evaporation component becomes important even at angles as small as 50^0 at low energy. This proves how necessary such an unfolding is, since no clear boundaries appear between the various reaction mechanisms even in an intermediate angular range (e.g. from 50^0 to 80^0).

Since fission is much more probable for gold than for silver a larger

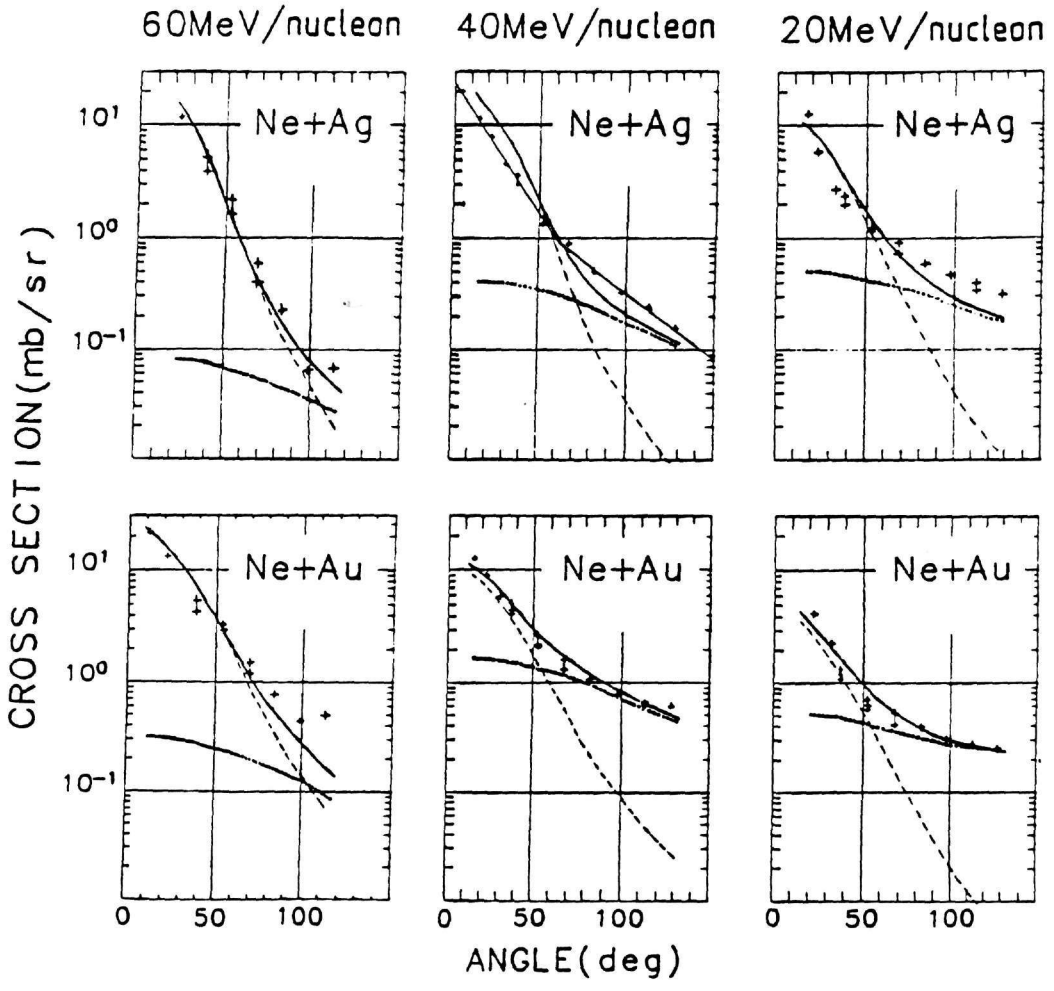

Figure 5: The angular distributions of Z=10 fragments (points) from Ne+Ag and Ne+Au in the range 20-60 MeV/nucleon are fitted (solid curves) by folding a component from intermediate-velocity source (dashed curves) with an evaporation contribution (dots).

equilibrated component is found for gold which makes the angular distributions smoother than those of silver. Even at 60 MeV/nucleon one observes a small detectable fission component which is almost absent for silver.

2.6 Cross sections for the nuclear fragmentation process

The cross section for each fragment was obtained by integrating the angular distributions of each fragment. The systematics of the cross sections for Z-separated fragments, integrated in the angular range $0^0 \leq \theta \leq 180^0$ are shown in fig. 6 for both reactions by dots (for more details see ref. [9,10,11]).

Cross sections for nuclear fragmentation are plotted versus Z in fig. 6 for both reactions (crosses). In the case of silver small differences are found with full angular range integrated cross sections. Exceptions occur for very light fragments owing to evaporation. Large discrepancies are on the contrary observed for gold beyond Z=10, especially for lower energies. making of the highest importance to remove the fission contribution from total cross sections. The evaporation- and fission- corrected total cross sections of fig. 6 appear distributed over Z-values in an almost energy independent way between 20 and 60 MeV/nucleon. To emphasize this important result all curves of fig. 6 have been parametrized in the form:

$$\sigma(Z) \propto Z^{-\tau} \tag{9}$$

where τ is an apparent (i.e. energy-dependent) exponent. If an increase of the beam energy is favoring the yield of the heaviest fragments , τ should decrease. Eventually it may have a minimum value. This is the trend predicted under the assumption of a phase transition in nuclear matter[12] or in percolation models[13]. In fig. 7 τ values extracted from Ne+Au uncorrected total cross sections[11] are plotted as a function of the largest available energy per nucleon calculated as $\frac{E^*_{max}}{A} = \sqrt{\frac{8E_{c.m.}}{A_{tot}}}$. They are decreasing from 20 to 40 MeV/nucleon whereas fragmentation cross sections for the same reaction give a nearly constant τ in the same domain. This shows that the decrease of τ at low energy is due to equilibrated

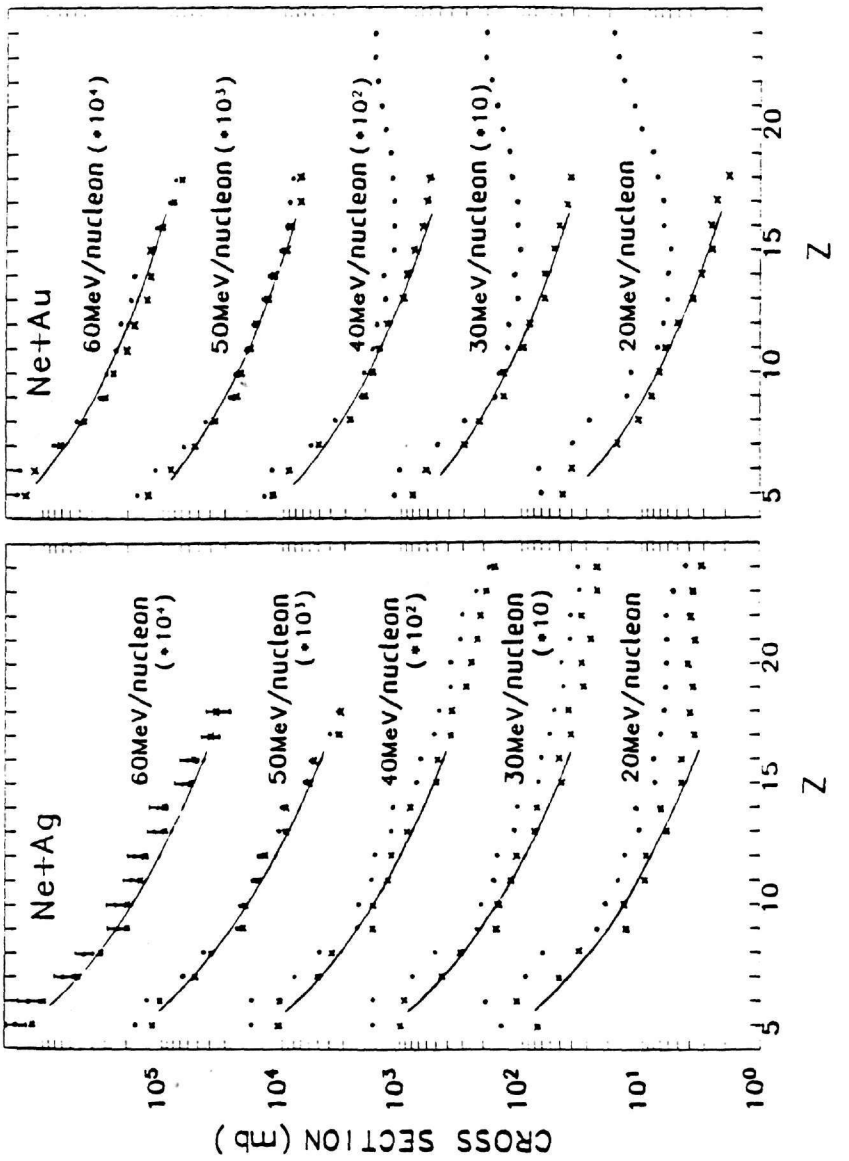

Figure 6: (Dots) Fragment yields for Ne+Ag and Ne+Au reactions at 20, 30, 40, 50 and 60 MeV/nucleon obtained by integrading the angular distributions in the range $0 \leq \theta \leq 180$ deg. (Crosses) Nuclear fragmentation cross sections extracted from the moving source analysis. Solid curves are power law fits.

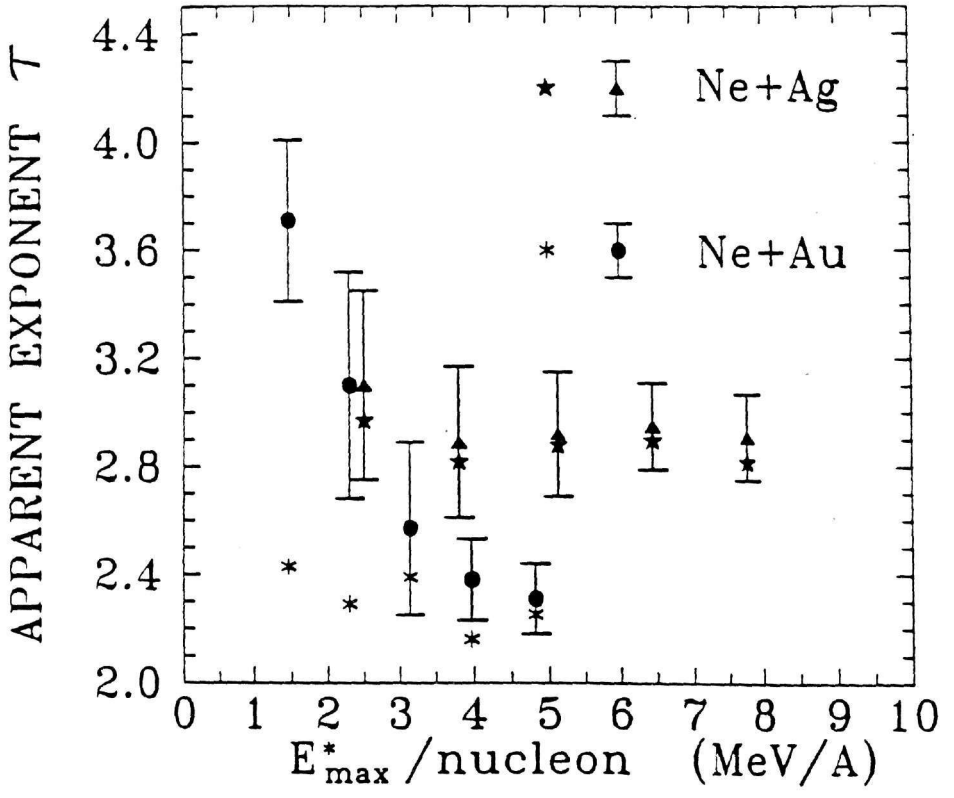

Figure 7: The apparent exponent τ as a function of the largest available energy per nucleon. Stars are for fragmentation data. Solid points and triangles are for the uncorrected cross sections. Errors on τ values from power law fits are $\leq$10%.

contributions (evaporation and fission). For Ne+Ag, from corrected and uncorrected [11] cross sections a small minimum hardly appears.

A further result is the important role of the target size since the asymptotic value of τ is larger for silver than for gold. One can indeed expect a smoother mass distribution (τ smaller) with a heavier target since a larger range of masses is available to the emitted fragments[14].

3 Conclusions

The inclusive IMFs obtained from the interaction of ^{20}Ne, from 20 to 60 MeV/nucleon incident energy, with silver and gold targets, enable us to make the following statements regarding the nature of their production.

Besides a strong projectile component at small angles ($\theta \leq 30$ deg.) for $Z \leq 10$, a contribution from evaporation exists with the silver target which decreases with energy. Most of the IMFs can be referred to nuclear fragmentation. Ne+Ag is a good reaction to choose for further investigation of this process.

For gold, in addition to the three above kinds of fragments there is an important component from asymmetric fission, the tail of which extends to lower Z-values with decreasing energy.

Some interesting features were found in the attempt to separate the fragmentation process from more relaxed mechanisms:

- A significant insensitivity of the process to the incident energy. This insensitivity made it possible to parametrize the fragmentation component at high energy where its contribution is dominant in the total cross section, then to reproduce in detail energy spectra and angular distributions at lower energies by adding to this high energy component increasing contributions from evaporation and fission.
- The same insensitivity to the beam energy is again evidenced by the fragments distributions through the constant value of τ, the exponent from the power law fit. This contrancy seems typical of the fragmentation process as soon as enough energy is available in a nuclear system to make it observable in an isolated investigation.
- Differences exist between Ne+Ag and Ne+Au reactions which emphasize the role of the size of the system: with the silver target the temperature of the fragmentation source decreases more strongly with the charge Z of the detected fragment and the asymptotic value of τ, the exponent from the power law fit, is larger.

References

[1] Proceedings of the 3rd International Conference on Nucleus-Nucleus Collisions. Saint-Malo, June 1988, Nucl. Phys. **A488**: Proceedings of the International Workshop on Nuclear Dynamics at Medium and High Energies, Bad Honnef. October 1988. Nucl. Phys. **A495** (1989); D.H.E. Gross. Rep. Prog. Phys. **53** (1990) 605; W.G. Lynch. Ann. Rev. Nucl. Part. Sci. **37** (1987) 493; C. Gregoire and T. Tamain Ann. Phys. Fr. 11 (1986) 323-455

[2] R. Dayras et al., Nucl. Phys. **A460** (1986) 299

[3] J. Aichelin. Phys. Rev. **C 30** (1984) 718

[4] D. J. Fields et al., Phys. Rev. **C 30** (1984) 1912

[5] V. E. Viola et al., Phys. Rev. **C 31** (1985) 1550

[6] J. Aichelin et al., Phys. Rev. **C 30** (1984) 107

[7] A. S. Hirsch et al., Phys. Rev. **C 29** (1984) 508

[8] G. Klotz-Engmann et al., Nucl. Phys. **A499** (1989) 392

[9] N. H. Papadakis et al., to be published in Phys. Rev. **C**

[10] "General characteristics of intermediate mass fragment inclusive cross sections in ^{20}Ne induced interactions" N. H. Papadakis et al., Contribution to this Symposium.

[11] N. H. Papadakis et al., Phys. Lett. **240B** (1990) 317

[12] A. D. Panagiotou et al., Phys. Rev. **C 31** (1985) 55

[13] X. Campi and J. Desbois. in Proceedings of the Topical Meeting on Phase Space Approach to Nuclear dynamics, Trieste, 1985

[14] H. W. Barz et al., Nucl. Phys. **A448** (1986) 753